In vivo and in vitro study on characterization and mechanism of the intestinal absorption of 2,3,5,4'-tetrahydroxy-stilbene-2-O-β-D-glucoside

Cheng Wang
Chengdu University of Traditional Chinese Medicine https://orcid.org/0000-0003-4731-8027
Yimeng Zhou
Chengdu University of Traditional Chinese Medicine
Xiaohong Gong
Chengdu University of Traditional Chinese Medicine
Li Zheng
Chengdu University of Traditional Chinese Medicine
Yunxia Li (lyxcdutcm@126.com)

Research article

Keywords: 2,3,5,4'-tetrahydroxystilbence-2-O-β-D-glucoside, Absorption mechanism, Caco-2 cell, Intestinal perfusion, P-gp, MRP2

Posted Date: October 3rd, 2019

DOI: https://doi.org/10.21203/rs.2.15497/v1

Version of Record: A version of this preprint was published on January 22nd, 2020. See the published version at https://doi.org/10.1186/s40360-020-0384-9.

Abstract

Background: 2,3,5,4'-tetrahydroxystilbence-2-O-β-D-glucoside(TSG) is a polyhydroxyphenolic compound, which exhibits a broad spectrum of pharmacological activities, such asanti-inflammatory, anti-depression, anti-oxidation and anti-atherosclerosis.However, the compound has poor bioavailability and the underlying absorption mechanisms has not been studied. Therefore, the purpose of this study was to investigate the intestinal absorption mechanism of TSG.

Methods: This study used the Caco-2 cell monolayer model and the single-passintestinal perfusion modelto explore the intestinal absorption mechanisms of TSG. The effects of basic parameters such as drug concentration, time and pH on the intestinal absorption of TSG were analyzed by high performance liquid chromatography.In addition, the susceptibility of TSG absorption process to treatment with three inhibitors, such as P-gp inhibitors verapamil hydrochloride and quinidine, and the MRP2 inhibitor probenecid were also assessed.

Results: TSG is poorly absorbed in the intestines and the absorption of TSG in the stomach is much higher than that in the intestine. Both in vivo and in vitro experiments showed that the absorption of TSG was saturated with increasing concentration. and it was better absorbed in a weakly acidic environment with a pH of 6.4. Moreover, TSG interacts with P-gp and MRP2, and TSG is not only the substrate of the P-gp and MRP2, but also affects the expression of P-gp and MRP2.

Conclusions: It can be concluded that the intestinal absorption mechanismsofTSG involve processes passive transport and the participation of efflux transporters.

Background

Polygonum multiflorum, is the dry root of *Polygonum multiflorum* Thunb. (Polygonaceae), which is wildly used as a nourishing Chinese medicine for it owning the pharmacological effects of neuroprotection, anti-oxidation, improving immunity, hypolipidemic, anti-atherosclerosis [1], anti-liver injury [2] and anti-cancer [3]. The chemical constituents of *Polygonum multiflorum* are complex, including stilbene glycosides, terpenoids, flavonoids, tannins, sugars and trace elements, in which 2,3,5,4’-tetrahydroxystilbene–2-O-β-D-glucoside (TSG) is the most effective active and the unique active ingredient. Modern studies have shown that TSG has a wide range of pharmacological effects, including anti-inflammatory [4], anti-depression [5], anti-oxidation [6], anti-atherosclerosis [7], improving gastrointestinal function [8] and protecting the cardiovascular system [9], etc. Clinically, TSG is used to prevent and treat hyperlipidemia [10], atherosclerosis [11], Alzheimer’s disease [12–13], Parkinson’s disease [14–15] and cerebral ischemia/reperfusion injury [16].

There are various routes of administration in clinic, and that of *Polygonum multiflorum* is mainly oral. It is prerequisite for drug efficacy.to be absorbed into the blood circulation system after oral administration. Our group have conducted pharmacokinetic studies on TSG, the main active ingredient of *Polygonum multiflorum.* However, results showed that the bioavailability of TSG was not high, indicating that only a

small amount of TSG entered the blood circulatory system. This discovery led us to have a strong interest in the absorption and metabolism of TSG in the gastrointestinal tract.

In order to reveal the influencing factors and mechanisms of oral drug absorption, researchers have established a variety of models, and the commonly used methods are Caco–2 cell model, in vivo intestinal perfusion model method, intestinal vascular intubation method and brush border membrane vesicle method [17–18]. Caco–2 cells are internationally recognized as a classic in vitro model for studying the absorption properties and transport mechanisms of oral drugs [19–20] because of their microvilli structure, biochemical properties similar to intestinal epithelial cells and enzymes associated with the intestinal brush epithelium, and expressing various transport proteins such as P-glycoprotein (P-gp) and multidrug resistance-associated protein 2 (MRP2). In vivo intestinal perfusion method is characterized by simple operation, mature technology and strong controllability, which can ensure the integrity of intestinal neuroendocrine regulation and the blood supply of lymph fluid [21]. It is also widely used to study the absorption of drugs in the intestine.

Therefore, this study combines the Caco–2 cell monolayer model and the single-pass intestinal perfusion model to study the factors affecting the absorption of TSG in intestine. In addition, in order to investigate the intestinal transport mechanism of TSG, western blotting was carried out to explore the effect of TSG on P-gp and MRP2 expression during absorption by administering P-gp inhibitors (verapamil hydrochloride and quinidine) and MRP2 inhibitor (probenecid). We hope this study will provide a reference for improving the bioavailability of TSG, designing a reasonable dosing regimen and predicting drug interactions.

Methods

2.1. Laboratory reagents

2,3,5,4’-tetrahydroxystilbence–2-O-β-D-glucoside (TSG, purity ≥ 98.72%), Rhaponticin (internal standard, IS, purity ≥ 98%), were obtained from Chengdu Chroma-Biotechnology Co., Ltd. Verapamil hydrochloride (purity ≥ 98%), quinidine (purity ≥ 98%), probenecid (purity ≥ 98%), were purchased from Chengdu Chroma-Biotechnology Co., Ltd. BCA protein quantification kit was purchased from Sichuan Sainst Biotechnology Co., Ltd. Anti-P glycoprotien antibody, Anti-MRP2 antibody, were purchased from Abcam, USA. Phenol red, GAPDH polyclonal antibody, purchased from Multisciences (Lianke) Biotech, co., Ltd. Ultrapure water (prepared by Yupu ultrapure water manufacturing system), HPLC-grade methanol, Phenol Red, acetonitrile, and formic acid (Fisher, USA).

2.2. Experimental instruments

Agilent 1260 High Performance Liquid Chromatograph (Agilent, USA); Flow Type Intelligent Peristaltic Pump (BT101L/G, Baoding Reef Fluid Technology Co., Ltd.); Electronic analytical balance (Sartorius 11D, Sartorius, Germany); Xiangyi desktop high-speed centrifuge (TG16-WS, Hunan Xiangyi Laboratory

Instrument Development Co., Ltd.); Ultrapure water meter (TANKPE030, Sichuan Yourun Technology Co., Ltd.); Carbon dioxide incubator (Forma 3111, Thermoscientific, USA); Purification workbench (SW-CJ–2FD, Suzhou Antai Air Technology Co., Ltd. Company); Ultrasonic Cell Crusher (SCIENTZ-IID, Ningbo Xinzhi Biotechnology Co., Ltd.); 12-well Polycarbonate Membrane Transfer Plate (3460 Transwell, Costar, USA, 0.4 μm pore size, 12 mm diameter, bottom area 1.12 cm^2); Electronic Constant Temperature Water Bath (DZKW–4, Beijing Zhongxing Weiye Instrument Co., Ltd.).

2.3. Caco–2 cell monolayer model

2.3.1. Cytotoxicity of TSG for Caco–2 cells.

MTT assay was used to investigate the effect of the target drug on Caco–2 cells before the transport experiment of TSG. Briefly, Caco–2 cells were seeded in 96-wells plates at a density of $1x10^4$ cells per well and placed in a carbon dioxide incubator. After 48 h incubation, the cells were treated with increasing concentrations of TSG (0.75–240 μg·mL^{-1}) and DMEM (containing 1%FBS) as a negative control. After 5 h of incubation, 20 μL of 5 mg·mL^{-1} MTT was added to each well, and the plate was incubated at 37 ℃ for 4 h. Then, the supernatant was aspired, and 150 μL of DMSO was added to each well. Absorbance was measured at a wavelength of 570 nm.

2.3.2. Caco–2 cell culture

Caco–2 cells (purchased from the Shanghai Cell Bank of the Chinese Academy of Sciences, passaged from 35 to 50 generations) were routinely cultured in DMEM which containing 20% FBS, 1% nonessential amino acids, 1% penicillin and 1% streptomycin at 37 ℃ in a humidified atmosphere. Subsequently, when the cells were grown to 80%–90%, 0.5 mL of the well-mixed Caco–2 cell suspension which at a cell density of $1x10^5$ cells·mL^{-1} was added to the AP side. On the 1st to 7th day of cell growth, the medium of AP and BL side were replaced with fresh DMEM on odd days. On the 8th to 14th day, the DMEM of double chamber were changed on odd days, and only the AP side was replaced on even days. After the 15th day, the medium of double chamber was changed every day. After 21 days of standardized culture, the morphology of Caco–2 cell monolayer was observed by electron microscopy and the cell monolayers with a TEER above 500 Ω·cm^{-2} were selected for transport assays. The membrane integrity and transport function of the Caco–2 cell monolayer model were further verified with propranolol hydrochloride and atenolol.

2.3.3. Absorption and transport of TSG on Caco–2 cell monolayer

Warmed HBSS (37 ℃) was used as the transport buffer for bidirectional transport, including absorption transport from the AP to the BL side and secretion transport from the BL to the AP side. Before transport studies, wash the cell monolayer three times with warm (37 °C) HBSS. In the transport experiment from

the AP side to the BL side, 0.5 mL of TSG solution at a concentration of 10, 30 or 60 μg·mL^{-1} was added to the AP side and 1.5 mL of HBSS was added to the BL side. On the contrary, in the transport experiment from the BL side to the AP side, 1.5 mL of TSG solution at a concentration of 10, 30 or 60 μg·mL^{-1} was added to the BL side and 0.5 mL of HBSS was added to the AP side. After administration, the transfer plate was placed in an incubator. Samples of 0.3 mL were taken on the BL side and samples of 0.1 mL were taken on the AP side at different time points (0.5, 1.0, 1.5, 2.0, 2.5, 3.0, 3.5 and 4.0 h). After each sampling, an equal volume of HBSS was added to the receiver chamber to maintain a constant volume. In addition, we also explored the transportation of TSG at different pH conditions (5.4, 6.4 and 7.4). The pH of DMEM (containing 1% FBS) was adjusted to 5.4 and 6.4, respectively, and TSG solutions of different pH were prepared for transport experiments to investigate the transport of TSG at different pH conditions.

2.3.4. Effects of P-gp and MRP2 on the absorption of TSG

The effect of efflux protein inhibitors on the intestinal absorption of TSG was studied based on the Caco–2 cell monolayer model. An appropriate amount of verapamil hydrochloride, quinidine and probenecid were accurately weighed and dissolved in DMEM to obtain an inhibitor solution with a concentration of 5 and 25 μg·mL^{-1}. Before the administration, the inhibitor was added to the AP side and BL side, and the plate was placed in an incubator. After 30 minutes, the inhibitor solution was replaced with a TSG solution at concentration of 30 μg·mL^{-1} to inspect the effect of efflux proteins on TSG.

2.3.5. Effect of TSG on the expression of P-gp and MRP–2

When Caco–2 cells were grown to 80%–90%, the cell were treated with different concentrations (10, 30 and 60 μg·mL^{-1}) of TSG and blank medium solution (as blank control group). After 4 h of incubation, the cell was treated with lysates, homogenized on ice for 10 min, centrifuged at 12 000 r·min^{-1} at 4 ℃ for 10 min., and then the supernatant was harvested. The concentration of total proteins was determined by BCA kit, and the supernatant were mix with SDS-PAGE sample buffer after protein quantification, denatured on a heater for 5 min and stored.

The total proteins were electrophoresed in 10% SDS-PAGE gel and then transferred to PVDF membranes by wet method to block with 5% skim milk for 2 h at room temperature. Membranes were incubated overnigh with the following primary antibodies Anti-P glycoprotein antibody (1:2000), Anti-MRP2 antibody (1:500), and GAPDH polyclonal antibody. After that, the membranes were washed with 0.1% TBST for 3 times and 10 min each time and incubated with corresponding secondary antibody (1:5000) for 1 h at room temperature. The OD density values of bands were analyzed using gel imaging and analysis system.

2.3.6. Determination of TSG by HPLC

HPLC conditions: Chromatographic separation was performed on Eclipse Plus C_{18} column (4.6 mm×250 mm, 5 μm). The column temperature was set at 30 °C. The mobile phase consisted of acetonitrile and 0.1% formic acid water (25:75) and the velocity of flow is 1 mL·min^{-1}. The injected sample volume was 5 μL. TSG was detected at wavelength of 320 nm. The samples were centrifuged at 12 000 r·min^{-}1 at 4 ℃ for 15 min. Then, the supernatant was analyzed by HPLC.

2.4. The intestinal perfusion in situ model

2.4.1. Experimental animal

Sprague-Dawley rats (200 ± 20 g) were supplied by the Animal Center of Chengdu University of TCM. All the rats were housed in a standard animal laboratory (23 ± 2 °C, relative humidity 50 ± 20%) with a 12 h light/dark cycle. Food was prohibited for 12 h before the experiment while water was provided freely. The animal experiments were conducted in accordance with Guide for the Care and Use of Laboratory Animals (NIH publication #85–23, revised in 1985). The Animal Ethics Committee of Chengdu University of Traditional Chinese Medicine (No.37 Twelve-bridge Road, Jinniu District, Chengdu, China) granted the experiment. The permission number was SCXK 2013–19.

2.4.2. Preparation of test solution

2.4.2.1. Preparation of artificial gastric juice. According to the Chinese Pharmacopoeia, the artificial gastric juice without pepsin is configured under the time limit inspection method of disintegration.

2.4.2.2. Preparation of gastric perfusate. The appropriate amount of TSG was accurately weighed, and the gastric perfusate was prepared at a concentration of 10, 30 and 60 μg·mL^{-1} using artificial gastric juice.

2.4.2.3. Preparation of Krebs-Ringer (K-R) buffer. Weigh $MgCl_2$: 0.02 g, NaCl: 7.80 g, KCl: 0.35 g, $NaHCO_3$: 1.37 g, NaH_2PO4: 0.32 g, in 1000 mL volumetric flask, add pure water to dissolve it fully, then 0.37 g of $CaCl_2$ was added while ultrasonication, and 1.40 g of Glucose was added at the time of use, sonicated, and the volume was adjusted with pure water to determine the pH of 7.4. All buffer solutions were prepared and used on the same day.

2.4.2.4. Preparation of blank intestinal circulating fluid. Accurately weigh the appropriate amount of phenol red, dissolve it with K-R buffer and dilute it into a phenol red solution with a mass concentration of 20 μg·mL^{-1}.

2.4.2.5. Preparation of intestinal circulation fluid. The proper amount of TSG was accurately weighed, and the intestinal circulation liquid with a concentration of 10, 30 and 60 μg·mL^{-1} was prepared by using a blank intestinal circulation solution.

2.4.3. In situ single-pass intestinal perfusion studies in rats

SD rats, half male and half female, were fasted for 12 hours but permitted to drink water freely before surgery. Rats were anesthetized by intraperitoneal injection of 25% urethane (0.05 $mL \cdot g^{-1}$) and placed in a supine position on the operating table. The abdominal cavity was opened along the midline of the abdomen, then the incision was made at the duodenum and the ileum. The polyethylene tubes were carefully inserted at both sides of the segment and ligatured with a sterile surgical line. The contents of the intestines were slowly rinsed with 0.9% saline, prewarmed at 37 °C, and the residual liquid in the intestine was drained with air. Afterward, the wound in the abdomen of the rats was covered with a gauze soaked with 37℃ 0.9% saline buffer to moisturize after the operation, warmed with infrared lamp. The intestinal was equilibrated with a drug-containing perfusate (the concentration of TSG was 10, 30 and 60 $\mu g \cdot mL^{-1}$ respectively) which was preheated at 37℃ at a flow rate of 5 $mL \cdot min^{-1}$. Samples were collected in EP tubes after 10 min, and blank intestinal circulation solution (1 mL) was quickly added to circulatory solution. After that, the flow rate was adjusted to 2 $mL \cdot min^{-1}$, and the samples were taken at 10 min intervals for 4 h. In addition, in order to study the effects of different pH on intestinal absorption of TSG, the pH of the blank intestinal circulation solution was adjusted to 5.4 and 6.4, respectively. Finally, the experimental animals were euthanized by the method of rapid decapitation when the experiment was over. The procedures and precautions for sacrifice were the same as previously described.

2.4.4. Effects of P-gp and MRP2 on the absorption of TSG

The effect of efflux protein inhibitors on the intestinal absorption of TSG was studied based on the intestinal recirculating perfusion model. The verapamil hydrochloride, quinidine and probenecid were dissolved in the blank intestinal circulation solution to obtain an inhibitor solution having a concentration of 25 and 5 $\mu g \cdot mL^{-1}$. The perfusion was started with inhibitor solution at a flow rate of 2 $mL \cdot min^{-1}$, and after 30 min, it was replaced with a TSG solution to investigate the influences of efflux proteins on TSG.

2.4.5. Determination of TSG by HPLC

HPLC conditions: Chromatographic separation was performed on Eclipse Plus C_{18} column (4.6 mm×250 mm, 5 μm). The column temperature was set at 30 °C. The mobile phase consisted of (A) 0.1% formic acid water and (B) acetonitrile. The gradient elution was set as: linear gradient elution 20–35% B (0–15min) with a flow rate of 1 $mL \cdot min^{-1}$. The injected sample volume was 5 μL. TSG was detected at wavelength of 320 nm and 430 nm. Samples of 1 mL were mix with equal amount of methanol, filtered through a membrane filter (0.45 μm pore size), and centrifuged at 12 000 $r \cdot min^{-1}$ for 10 min, then the concentration of TSG and phenol red of supernatant were measured by HPLC. The concentration of phenol red was used to correct the volume of intestinal circulating fluid. According to the concentration of TSG and the volume of intestinal circulating fluid in each time period, the residual drug amount (X) in the intestinal circulatory fluid was calculated, and the sampling time t was plotted as a line with lnX, and the

absorption was determined from the slope of the straight line. Rate constant Ka. The percentage of drug absorption in the time period was determined by the ratio of the change value of the remaining dose of t (h) to the amount of the remaining drug at time 0.

2.5. Data analysis

The effective permeability coefficient (P_{app}, cm/s) across Caco–2 cell monolayer was calculated from the linear plot of drugs accumulated in the receiver side versus time using the following equation (1):

$$P_{app} = dQ/dt \times 1/A \times 1/C_0 \quad (1)$$

Where dQ/dt represents the steady-state flux of the drug on the receiver (serosal in the case of AP-BL side studies or mucosal in the case of BL-AP side studies) side, C_0 is the initial concentration of the compound in the donor side, and A is the surface area of the polycarbonate membrane.

Since the HBSS buffer was added after each sampling to dilute the drug concentration, the cumulative absorption concentration (C_{cum}) of the drug was corrected using the following equation (2):

[Due to technical limitations, this equation is only available as a download in the supplemental files section.]

where C_{cum} represents the cumulative concentration of the drug, A_n represents the permeation concentration of the nth sample, V_n represents the sampling volume of the nth sample, and V represents the volume of the receiving pool.

The absorption rate constants (Ka) and percentage of absorption (PA, %) were calculated using the following equations (3), (4), respectively.

$$\ln X = \ln XO - Ka \cdot t \quad (3)$$

$$PA = (C_0V_0 - C_tV_t)/C_0V_0t \times 100\% \quad (4)$$

Where X is the residual drug amount, C_0 is the drug concentration of intestinal circulation liquid at 0 min, V_0 is the drug volume of intestinal circulation liquid at 0 min, C_t is the drug concentration of intestinal circulation liquid at t min, V_t is the drug volume of intestinal circulation liquid at t min, t is the perfusion time.

2.6. Statistical analysis

All experiments were performed in triplicate (minimum) and results were expressed as the mean ± SD. Statistical comparisons were performed by one-way analysis of variance (ANOVA) using SPSS 21.0. When $p < 0.05$, it was considered statistically significant. All data were represented for at least three independent experiments.

Results

3.1. Caco–2 cell monolayer model

3.1.1. The results of the cytotoxicity test

In order to avoid the false positive result of the target drug on the cells, we examined the effect of the target drug on cell viability by MTT assay before the transport experiment. The results are shown in Fig. 2. The cell viability in the presence of 60 μg·mL^{-1} TSG was greater than 90%. When the concentration of TSG was more than 60 μg·mL^{-1}, the cell viability was significantly decreased. Hence, transportation studies were conducted at concentrations of 10, 30, and 60 μg·mL^{-1} TSG.

3.1.2. The characterization of Caco–2 cell monolayer

The integrity of the Caco–2 cell monolayer was evaluated by measuring TEER and transport studies of propranolol hydrochloride and atenolol, an internationally recognized positive control. In our data, Caco–2 cell monolayer displayed a TEER value high than500 Ω·cm^{-2} after 21 days of culture in the transfer plate. Propranolol hydrochloride and atenololl showed different absorption in the Caco–2 cell monolayer model. The results of transport experiments showed that the P_{app} values of the AP-BL of propranolol hydrochloride on this model was (1.56 ± 0.24) × 10^{-5} cm·s^{-1}, and the P_{app} values of the AP-BL of atenolol was (5.82 ± 1.25) × 10^{-7} cm·s^{-1}, which were in a good agreement with the P_{app} reported in the literature. These results indicate that Caco–2 cell monolayer model has tight junction and transport capacity and can be used for transport experiments.

3.1.2. The characterization of the intestinal permeability features of TSG

A Caco–2 cell monolayer model was used to explore the intestinal permeability features of TSG. Firstly, the P_{app} values were measured at different TSG concentrations (10, 30 and 60 μg·mL^{-1}). It was found that the P_{app} values of TSG were between 1 × 10^{-6} and 10 × 10^{-6} cm/s, which was also between propranolol hydrochloride and atenolol. This indicates that TSG is a moderately absorbed drug. As shown in Fig. 3A, the bilateral (AP-BL and BL-AP) P_{app} TSG decreased substantially with increasing concentration and remained basically unchanged after reaching a certain concentration. In the bidirectional transport experiment, there was a significant difference between low concentrations and medium and high concentrations ($p < 0.05$). However, no significant difference was found between medium concentrations and high concentrations of TSG ($p > 0.5$). Furthermore, the P_{app} values obtained after incubation with TSG for 1, 2, 3 and 4 h across Caco–2 cell monolayer in the AP-BL and BL-AP direction is presented in Fig. 3B and Fig. 3C. It was found that the absorption of TSG on the Caco–2 cell

monolayer model did not have time-dependent. The bilateral P_{app} values of different concentrations of TSG reached the maximum at 1 h after administration, and gradually decreased to a steady state with the prolongation of time. TSG absorbs rapidly in the Caco–2 cell monolayer model, and as the concentration increases, the absorption gradually becomes saturated. This indicates that the transport of TSG may be transported by carrier protein on the cell model.

Subsequently, the pH of DMEM (containing 1% FBS) was adjusted to 6.4 and 5.4, respectively, and formulated into TSG solutions of different pH. The effects of different pH values on TSG transport at a concentration of 30 $\mu g \cdot mL^{-1}$ are shown in Fig. 3D. P_{app} values of TSG bidirectional transport increased significantly with the decrease of pH value. The bidirectional P_{app} value of TSG at pH 6.4 and 5.4 were significantly higher than that the P_{app} value at pH 7.4 (p <0.05). However, there was no significant difference between the P_{app} value of the pH 6.4 and the pH 5.4 (p > 0.05). Our data demonstrate that the transport of TSG may be affected by acidic conditions. Simultaneously, it also shows that the weakly acidic conditions at pH 6.4 is more conducive to the absorption of TSG.

3.1.3. The role of P-gp and MRP2 on TSG transport across Caco–2 cell monolayer

Next, we also speculated that the efflux transporter plays an important role in the permeability of TSG through the Caco–2 cell monolayer as shown in Fig. 4. Compared with treatment using TSG alone, for the co-treatment with 5 $\mu g \cdot mL^{-1}$ P-gp inhibitor (verapamil hydrochloride and quinidine) and MRP2 inhibitor (probenecid), the P_{app} values of TSG increased about 2.68 times (p < 0.01), 2.74 times (p < 0.01) and 2.22 times (p < 0.01), respectively on the AP-BL side and 1.14 times, (p > 0.05) 1.26 times (p < 0.05) and 1.82 times (p < 0.01), respectively on the BL-AP side. Similarly, compared with treatment using TSG alone, for the co-treatment with 25 $\mu g \cdot mL^{-1}$ P-gp inhibitor (verapamil hydrochloride and quinidine) and MRP2 inhibitor (probenecid), the P_{app} values of TSG increased about 4 times (p < 0.01), 3.18 times (p < 0.01) and 3.02 times (p < 0.01), respectively, on the AP-BL side and 1.88 times (p < 0.01), 1.51 times (p < 0.01) and 1.91 times (p < 0.01), respectively on the BL-AP side. These results indicate that verapamil hydrochloride, quinidine and probenecid can promote the absorption of TSG, suggesting that P-gp and MRP2 mediate the transport of TSG. Therefore, the in vitro transport data indicates that TSG may be the substrate of the efflux protein P-gp and MRP2.

3.1.4. Effects of TSG on the expression of P-gp and MRP2 in Caco–2 cell monolayer

The results of western blotting experiments are shown in Fig. 5. After incubation with different concentrations of TSG (10, 30 and 60 $\mu g \cdot mL^{-1}$, respectively), the expression of P-gp in Caco–2 cells increased, and there was a significant difference at 60 $\mu g \cdot mL^{-1}$ ($p < 0.05$). However, the expression of MRP2 in cells was decreased, and the inhibitory effects of 60 and 30 $\mu g \cdot mL^{-1}$ of TSG were significant (p

< 0.05). TSG are capable of inducing P-gp expression but inhibiting MRP2 expression. It can be seen that TSG is not only affected by P-gp and MRP2, but also affects the expression of efflux proteins, and there is an interaction during transport.

3.2 Single-pass intestinal perfusion in suit model

3.2.1. The characterization of the intestinal permeability features of TSG in rats

The single-pass intestinal perfusion model was used to further explore the intestinal permeability features of TSG in rats. Firstly, we determined the absorption of different concentrations (10, 30 and 60 $\mu g \cdot mL^{-1}$) of TSG in the stomach. These results showed that TSG was well absorbed in the stomach, and the absorption in the stomach increased significantly with the increase of concentration ($P < 0.05$), which showed a passive transport mechanism.

Subsequently, we measured the percentage of absorption (PA, %) values and absorption rate constants (Ka, h^{-1}) values of TSG at different drug concentrations (10, 30 and 60 $\mu g \cdot mL^{-1}$) and the results are shown in Fig. 6A and Fig. 6B. The PA and Ka of TSG of 10 $\mu g \cdot mL^{-1}$ were significantly greater than the drug concentration at 30 and 60 $\mu g \cdot mL^{-1}$ ($p < 0.05$). However, there was no significant difference between medium and high concentrations ($p > 0.05$). The absorption of TSG in the small intestine remains unchanged after the concentration increases to a certain value, and the absorption is saturated. Hence, it is speculated that TSG is mainly absorbed into the blood circulation system through carrier transport.

The Ka and PA values of TSG were measured at different pH values (7.4, 6.4 and 5.4). As shown in Fig. 6C and Fig. 6D, the Ka of TSG showed a significant increase between the group with pH 6.4 and 7.4 ($p < 0.01$), the PA value of the control group with pH 7.4 was significantly different from the other two groups ($p < 0.05$). In other words, TSG shows better absorption in a weakly acidic environment.

3.2.2. The role of P-gp and MRP2 on intestinal permeability of TSG

To further confirm the role of P-gp and MRP2 on the intestinal permeability of TSG, the Ka and PA values were measured in the presence of verapamil hydrochloride, quinidine and probenecid protein inhibitors. As the findings in Fig. 7 indicate, the Ka and PA values of TSG were measured in the presence of verapamil hydrochloride and quinidine. The results indicate that the Ka and PA values of TSG increased significantly ($p < 0.05$) with inhibitor of P-gp at concentration of 25 $\mu g \cdot mL^{-1}$. The absorption of TSG in the intestine increases with the concentration of inhibitor, it indicates that P-gp mediates the intestinal epithelium transportation of TSG, and it is speculated that TSG is a substrate of P-gp.

The MRP2 inhibitor, probenecid, can enhance the permeability of TSG in the intestine, the Ka and PA values of TSG were significantly different from control group without inhibitor when the concentration of

probenecid is 25 μg·mL^{-1} ($p < 0.05$). The result shown that the intestinal permeability of TSG was limited by MRP2. Therefore, the in vivo transport data also indicates that TSG may be the substrate of the efflux protein P-gp and MRP2.

Discussions

TSG, also named 2,3,5,4'-tetrahydroxystilbence–2-O-β-D-glucoside, is a unique active component of Polygonum multiflorum. As a quality control index specified in the Pharmacopoeia of the People's Republic of China, TSG possesses various effects, including anti-aging, lowering blood lipids, anti-atherosclerosis, anti-tumor and liver protection [6–9]. Previously, studies have evaluated the pharmacokinetics, tissue uptake, distribution and excretion of TSG systematically, all of which indicated a poor bioavailability and low tissue exposure of TSG. For example, Zhao et al [22] determined TSG concentration in plasma in rats using LC-Q-TOF-MS. According to the fitting analysis of two-compartment model, the maximal concentration of TSG (C_{max}) was 5.70 μg·mL^{-1}, indicating that only a small amount of TSG was absorbed, the absorption half-life (t1/2Ka) was 14.80 min, indicating that TSG can be absorbed rapidly in vivo. The results are consistent with the conclusions of noncompartmental analysis of Lv et al [23–24]. However, there are few studies on the low bioavailability of TSG in vivo, and the absorption mechanisms in the gastrointestinal tract are yet to be clarified. Therefore, this study aims to interpret the absorption characteristics and its potential mechanism of TSG in the intestine both in vitro and in vivo.

Polygonum multiflorum and its preparations are mostly administered orally in clinic. Thus, it is of great significance to investigate whether the main components of TSG are absorbed and its absorption characteristics. Oral administration is the most common and convenient way of administration, and the absorption of drugs in the intestine is a transmembrane transport process. Therefore, the intestinal absorption characteristics of drugs are one of the decisive factors for efficacy, accurate and efficient evaluation of the permeability of components has become a great challenge in the development of new drugs. Caco–2 cell is an international recognized drug absorption model which is widely used in drug research and development, and it is reported that there is a certain correlation between transportation and absorption of drugs in vivo [25]. In this study, we examined the effect of TSG on cell viability by MTT assay before the transport experiment, which helps to eliminate the influence of toxicity of TSG on the cells. MTT assay is a commonly used method for detecting cell growth, cell activity and cytotoxicity. In our study, the results of MTT assay showed that TSG had basically no toxicity on Caco–2 cells within the concentrations of 0.75–60 μg·mL–1. Therefore, subsequent transport experiments were conducted at concentrations of 10, 30, and 60 μg·mL–1 TSG.

In the Caco–2 cell monolayer model, our data showed that the P_{app} value of TSG between 1.0×10^{-6} and 10.0×10^{-6} cm·s^{-1}, which indicates TSG is absorbed moderately and has a low permeability in vitro according to the internationally accepted standard for drug absorption. The results of cell transfer assay showed that the absorption of TSG in Caco–2 cell model did not have time-dependent, and the P_{app}

values of TSG bidirectional transport at different concentrations all reached the maximum at 1 h. With the prolongation of time, the P_{app} values of TSG gradually decreases and tended to balance. It suggests that the transport of TSG in the intestine mainly rely on carrier proteins. In addition, the transport results of TSG at different pH conditions showed that the P_{app} values increased significantly with the decreasing of pH, and it showed a better absorption in the weakly acidic conditions at pH 6.4.

On the other hand, in the single-pass intestinal perfusion model, our results showed that the absorption of TSG in the stomach is much higher than that in the intestine. TSG has an increased absorption in the stomach with increasing concentrations, which showed a passive transport absorption mechanism. However, the absorption of TSG in the intestine decreased when concentration increases and showed a saturation phenomenon when the concentration reaches a certain value, which was transported by the help of carrier proteins and showed a promotion diffusion. The results are consistent with the transport experiments in vitro. Interestingly, we also found that in a single-pass intestinal perfusion model, TSG also showed a better absorption in the weakly acidic conditions at pH 6.4. The reason may be that TSG contains multiple phenolic hydroxyl groups, which are mainly present in molecular form in the acidic conditions and have good lipid solubility. The absorption increases in the weakly acidic conditions at pH 6.4, which may account for the transport mechanism of dissolution diffusion.

The process of drug absorption in the body is complicated and is affected by many factors, such as the physical and chemical properties of drug, the gastrointestinal environment, and the transporter on the intestinal tract [26]. A variety of transporters are expressed on the membrane of intestinal epithelial cells, among which the outward transporter (efflux protein) can actively discharge drugs from cells, which lead to the reduction of drug absorption. In recent years, efflux protein-mediated drug efflux has attracted extensive attention. The efflux protein is an energy-dependent protein widely distributed in various tissues of the body [27], mainly mediating the absorption, distribution, metabolism and excretion of drugs [28]. P-gp, MRP2 and breast cancer resistance protein (BCRP) are the major efflux proteins. Meanwhile, P-gp and MRP2 are highly expressed in the intestine and have been studied extensively at present. P-gp and MRP2 are distributed in the brush border of intestinal mucosal epithelial cells. The expression of P-gp is gradually increased from the proximal to the distal of the intestine. However, MRP2 is expressed mainly in the jejunum, which plays a key role in drug absorption. P-gp and MRP2 belong to the ABC family transporters and contain one or two ATP-binding regions in the molecule. The energy produced by ATP decomposition can be directly utilized to drain intracellular drugs out of cells, resulting in reduced drug absorption and bioavailability. Therefore, the addition of inhibitors can inhibit the exocytosis of efflux proteins and promote the absorption and distribution of drugs.

Results of infusion experiments in vitro and in vivo both indicated that the addition of P-gp inhibitors (verapamil hydrochloride and quinidine) and MRP2 inhibitor (probenecid) increased the absorption of TSG, indicating P -gp and MRP2 inhibitors can significantly increase the permeability of TSG in the intestinal epithelium. These results show that P-gp and MRP2 proteins are involved in the absorption of TSG, suggesting that TSG may be a substrate of efflux proteins P-gp and MRP2. In other words, in

addition to passive transport, there is also an efflux protein-mediated primary active transport mechanism. The intestinal permeability of TSG may, at least partly, be limited by P-gp and MRP2.

In addition to the efflux proteins, metabolic enzymes also play a very important role in the intestinal absorption of drugs [29]. A variety of enzymes related to drug metabolism are expressed in the intestine, such as CYP450, glucuronyltransferase, N-acetyltransferase, glutathione S-transferase and esterase. In the process of intestinal transport, the enzymes of drug metabolism bind to the substrate, forming a metabolite, and the drug absorption is reduced due to the intestinal first pass effect. CYP3A4 is the most important enzyme in the CYP450 family and is involved in intestinal metabolism of approximate 90% drugs. Studies have shown that verapamil hydrochloride can not only inhibit the efflux of P-gp protein, but also inhibit the expression of CYP3A4, which can reduce the metabolism of substrates [30]. Verapamil hydrochloride can promote the absorption of TSG, and we hypothesized that in addition to inhibit P-gp protein, verapamil hydrochloride may also inhibit the metabolism of TSG by CYP3A4, thereby increasing intestinal absorption. Therefore, the impact of drug-metabolizing enzymes on TSG remains to be further studied.

Although this study combines in vitro Caco–2 cell transport experiments and in vivo gastrointestinal perfusion experiments to systematically study the absorption mechanism of TSG in the gastrointestinal tract, the current study still suffers from certain limitations. For example, our study found that TSG showed moderate absorption in the Caco–2 cell monolayer model. According to the cell model for drug absorption, it is predicted that its absorption in the intestine should be 20%–70%. However, the absorption rate obtained in our study was significantly lower than 20%, and the results of the two models were different. Caco–2 cell monolayer model lacks mucus layer and some metabolic enzymes in intestinal wall, and the barrier characteristics are different from those of small intestinal epithelial cells. Therefore, it may lead to some differences in transport in vitro and in vivo experiment.

In summary, our study showed that TSG has a low permeability in intestinal epithelial cells. Additionally, we also found that intestinal absorption of TSG involves promoting passive diffusion and may be affected by the efflux transporters P-gp and MRP2. In future studies, we will focus on the effects of intestinal microflora, other transporters and metabolic enzymes on the intestinal absorption mechanism of TSG.

Conclusions

In this study, we investigated the effects of different concentrations, time, PH and transporter inhibitors on the absorption of TSG in the Caco–2 cell model and in single-pass intestinal perfusion model. The present study has revealed that TSG is poorly absorbed in the intestines. Both in vivo and in vitro experiments showed that the absorption of TSG was saturated with increasing concentration, and it was better absorbed in a weakly acidic environment with a pH of 6.4. In other words, it is suggested that the absorption mechanism of TSG in the intestine is passive transport. In addition, we have also found that the intestinal absorption mechanism of TSG may involve facilitated passive diffusion associated with

the efflux transporters P-gp and MRP2. As a whole, during the transport process, TSG interacts with P-gp and MRP2, and TSG is not only the substrate of the P-gp and MRP2, but also affects the expression of P-gp and MRP2. In conjunction with results from previous studies along the direction of TSG, these results provide updated information concerning the intestinal absorption process and the possible mechanism of this compound.

Abbreviations

TSG: 2,3,5,4'-tetrahydroxystilbence–2-O-β-D-glucoside; P-gp: P-glycoprotein; MRP2: Multidrug resistance-associated protein 2; DMEM: Dulbecco's modified eagle medium; FBS: Fetal bovine serum; MTT: Methylthiazolyldiphenyl-tetrazolium bromide; TEER: Trans-epithelial electrical resistance; HPLC: High performance liquid chromatography; HBSS: Hank's banlanced salt solution; PBS: Phosphate buffered saline; GAPDH: Glyceraldehyde–3-phosphatedehydrogenase; P_{app}: Apparent absorption coefficient; K_a: Absorption rate constant; PA: Percentage of absorption; C_{cum}: cumulative absorption concentration

Declarations

1. Ethics approval and consent to participate

The animal experiments were conducted in accordance with Guide for the Care and Use of Laboratory Animals (NIH publication #85–23, revised in 1985). The Animal Ethics Committee of Chengdu University of Traditional Chinese Medicine (No.37 Twelve-bridge Road, Jinniu District, Chengdu, China) granted the experiment. The permission number was SCXK 2013–19.

2. Consent for publication

Not applicable.

3. Availability of data and materials

The datasets used and/or analysed during the current study are available from the corresponding author on reasonable request.

4. Competing interests

The authors declare that they have no competing interests.

5. Funding

The research was supported by National Natural Science Foundation of China (Grant No. 81373943, 81573583) and Sichuan Provincial Science and Technology Department of Youth Science and technology innovation research team program (Grant No. 2017TD0001, 2016TD007). The funding sources played no role in, nor influenced study design, data collection, data analysis, data interpretation, or preparation of the manuscript.

6. Authors' contributions

CW wrote and substantively revised the manuscript; YZ and LZ performed the experiments; XG analyzed the data; YL acted as a supervisor obtained the funding.

7. Acknowledgements

Not applicable.

8. Authors' information

[1] College of Pharmacy, Chengdu University of Traditional Chinese Medicine, Chengdu 611137, China

References

[1] Bounda GA, Feng YU. Review of clinical studies of *Polygonum multiflorum* Thunb. and its isolated bioactive compounds. Phcog Res. 2015;7(3):225–236.

[2] Lin L, Ni B, Lin H, Zhang M, Li X, Yin X, Qu C, Ni J. Traditional usages, botany, phytochemistry, pharmacology and toxicology of *Polygonum multiflorum* Thunb.: A review. J Ethnopharmacol. 2015;159:158–183.

[3] Zong A, Cao H, Wang F. Anticancer polysaccharides from natural resources: a review of recent research. Carbohydr Polym. 2012;90(4):1395––1410.

[4] Zhao J, Liang Y, Song F, Xu S, Nian L, Zhou X, Wang S. TSG attenuates LPC-induced endothelial cells inflammatory damage through notch signaling inhibition. Iubmb Life. 2016;68(1):37–50.

[5] Jiang C, Qin X, Yuan M, Lu G, Cheng Y. 2,3,5,4'-Tetrahydroxystilbene–2-O-beta-D-glucoside Reverses Stress-Induced Depression via Inflammatory and Oxidative Stress Pathways. Oxid Med Cell Longev. 2018;2018:9501427.

[6] Jiang Z, Wang W, Guo C. Tetrahydroxy stilbene glucoside ameliorates H2O2-induced human brain microvascular endothelial cell dysfunction in vitro by inhibiting oxidative stress and inflammatory responses. Mol Med Rep. 2017;16(4):5219–5224.

[7] Yao W, Huang C, Sun Q, Jing X, Wang H, Zhang W. Tetrahydroxystilbene glucoside protects against oxidized LDL-induced endothelial dysfunction via regulating vimentin cytoskeleton and its colocalization with ICAM–1 and VCAM–1. Cell Physiol Biochem. 2014;34(5):1442–1454.

[8] Wu J, Hu W, Gong Y, Wang P, Tong L, Chen X, Chen Z, Xu X, Yao W, Zhang W, Huang C. Current pharmacological developments in 2,3,4',5-tetrahydroxystilbene 2-O-β-D-glucoside (TSG). Eur J Pharmacol. 2017;811:21–29.

[9] Yamamoto M, Clark JD, Pastor JV, Gurnani P, Nandi A, Kurosu H, Miyoshi M, Ogawa Y, Castrillon DH, Rosenblatt KP, Kuro-o M. Regulation of oxidative stress by the anti-aging hormone klotho. J Biol Chem. 2005;280(45):38029–38034.

[10] Wang W, He Y, Lin P, Li P, Li Y, Sun R, Gu W, Yu J, Zhao R. In vitro effects of active components of Polygonum Multiflorum Radix on enzymes involved in the lipid metabolism. J Ethnopharmacol. 2014;153(3):763–770.

[11] Chen X, Tang K, Peng Y, Xu X. 2, 3, 4', 5-tetrahydroxystilbene–2–0-β-D glycoside attenuates atherosclerosis in apolipoprotein E-deficient mice: role of reverse cholesterol transport. Can J Physiol Pharmacol. 2018;96(1):8–17.

[12] Zhang RY, Zhang L, Zhang L, Wang YL, Li L. Anti-amyloidgenic and neurotrophic effects of tetrahydroxystilbene glucoside on a chronic mitochondrial dysfunction rat model induced by sodium azide. J Nat Med. 2018;72(3):596–606.

[13] Jiao C, Gao F, Ou L, Yu J, Li M, Wei P, Miao F. Tetrahydroxy stilbene glycoside (TSG) antagonizes Aβ-induced hippocampal neuron injury by suppressing mitochondrial dysfunction via Nrf2-dependent HO–1 pathway. Biomed pharmacother. 2017;96:222–228.

[14] Zhang R, Sun F, Zhang L, Sun X, Li L. Tetrahydroxystilbene glucoside inhibits α-synuclein aggregation and apoptosis in A53T α-synuclein-transfected cells exposed to MPP. Can J Physiol Pharmacol. 2017;95(6):750–758.

[15] Zhang L, Huang L, Li X, Liu C, Sun X, Wu L, Li T, Yang H, Chen J. Potential molecular mechanisms mediating the protective effects of tetrahydroxystilbene glucoside on MPP-induced PC12 cell apoptosis. Mol Cell Biochem. 2017;436:203–213

[16] Mu Y, Xu Z, Zhou X, Zhang H, Yang Q, Zhang Y, Xie Y, Kang J, Li F, Wang S. 2,3,5,4'-Tetrahydroxystilbene–2-O-β-D-glucoside attenuates ischemia/reperfusion-induced brain injury in rats by promoting angiogenesis. Planta Med. 2017;83(08):676–683.

[17] Gurunath S, Nanjwade BK, Patila PA. Enhanced solubility and intestinal absorption of candesartan cilexetil solid dispersions using everted rat intestinal sacs. Saudi Pharm J. 2014;22(3):246–257.

[18] Wang X, Liu G, Yang Y, Wu X, Xu W, Yang X. Intestinal absorption of triterpenoids and flavonoids from glycyrrhizae radix et rhizoma in the human caco–2 monolayer cell model. Molecules. 2017, 22(10):1627.

[19] Artursson P, Palm K, Luthman K. Caco–2 monolayers in experimental and theoretical predictions of drug transport. Adv Drug Deliv Rev. 2012;64(1–2):280–289.

[20] Zhang D, Lei T, Lv C, Zhao H, Xu H, Lu J. Pharmacokinetic studies of active triterpenoid saponins and the total secondary saponin from anemone raddeana regel. J Chromatogr B Analyt Technol Biomed Life Sci. 2017;1044–1045:54–62.

[21] Xin L, Liu XH, Yang J, Shen HY, Ji G, Shi XF, Xie Y. The intestinal absorption properties of flavonoids in Hippophaë rhamnoides extracts by an in situ single-pass intestinal perfusion model. J Asian Nat Prod Res. 2019;21(1):62–75.

[22] Zhao Y, Zhang L, Feng Y, Chen D, Xi Z, Du X, Bai X, Lin R. Pharmacokinetics of 2,3,5,4'-tetrahydroxystilbene-2-O-β-D-glucoside in rat using ultra-performance LC-quadrupole TOF-MS. J Sep Sci. 2013;36(5):863–871.

[23] Lv G, Gu H, Chen S, Lou Z, Shan L. Pharmacokinetic profile of 2,3,5,4’-tetrahydroxystilbene–2-O-β-D-glucoside in mice after oral administration of Polygonum multiflorum extract. Drug Dev Ind Pharm. 2012;38(2):248–255.

[24] Lv G, Lou Z, Chen S, Gu H, Shan L. Pharmacokinetics and tissue distribution of 2,3,5,4’-tetrahydroxystilbene–2-O-Î²-D-glucoside from traditional Chinese medicine Polygonum multiflorum following oral administration to rats. J Ethnopharmacol. 2011;137(1):449–456.

[25] Stappaerts J, Brouwers J, Annaert P, Augustijns P. In situ perfusion in rodents to explore intestinal drug absorption: challenges and opportunities. Int J Pharm. 2015;478(2):665–681.

[26] Ayrton A, Morgan P. Role of transport proteins in drug absorption, distribution and excretion. Xenobiotica. 2001;31(8–9):469–497.

[27] Maubon N, Le Vee M, Fossati L, Audry M, Le Ferrec E, Bolze S, Fardel O. Analysis of drug transporter expression in human intestinal Caco–2 cells by real-time PCR. Fundam Clin Pharmacol. 2007;21(6):659–663.

[28] Borlak J, Zwadlo C. Expression of drug-metabolizing enzymes, nuclear transcription factors and ABC transporters in Caco–2 cells. Xenobiotica. 2003;33(9):927–943.

[29] Ahmmed SM, Mukherjee PK, Bahadur S, Harwansh RK, Kar A, Bandyopadhyay A, Al-Dhabi NA, Duraipandiyan V. CYP450 mediated inhibition potential of Swertia chirata: an herb from Indian traditional medicine. J Ethnopharmacol. 2016;178:34–39.

[30] Kapetas AJ, Sorich MJ, Rodrigues AD, Rowland A. Guidance for rifampin and midazolam dosing protocols to study intestinal and hepatic cytochrome P450 (CYP) 3A4 induction and de-induction. AAPS J. 2019;21(5):78.

Figures

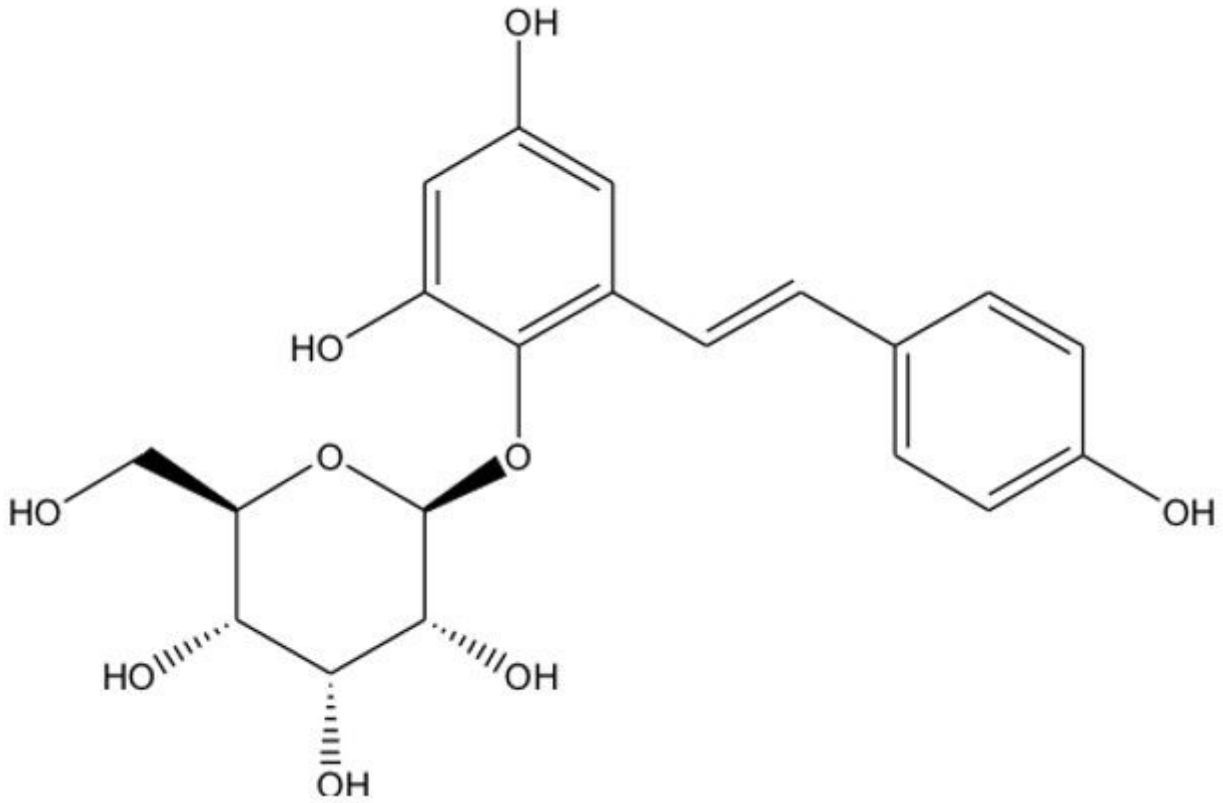

Figure 1

Chemical structure of TSG

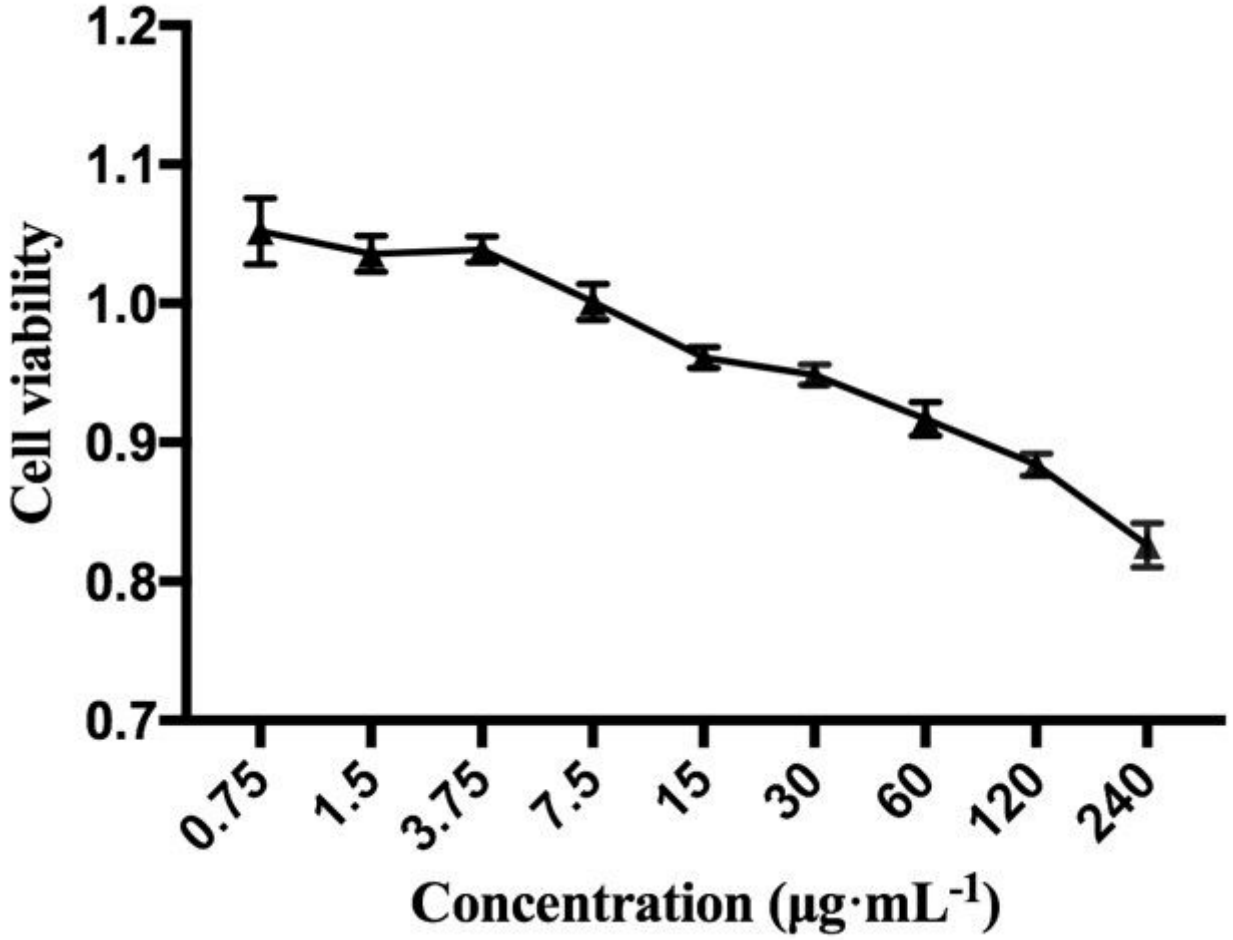

Figure 2

Cell viability of TSG on Caco-2 cells (n = 3)

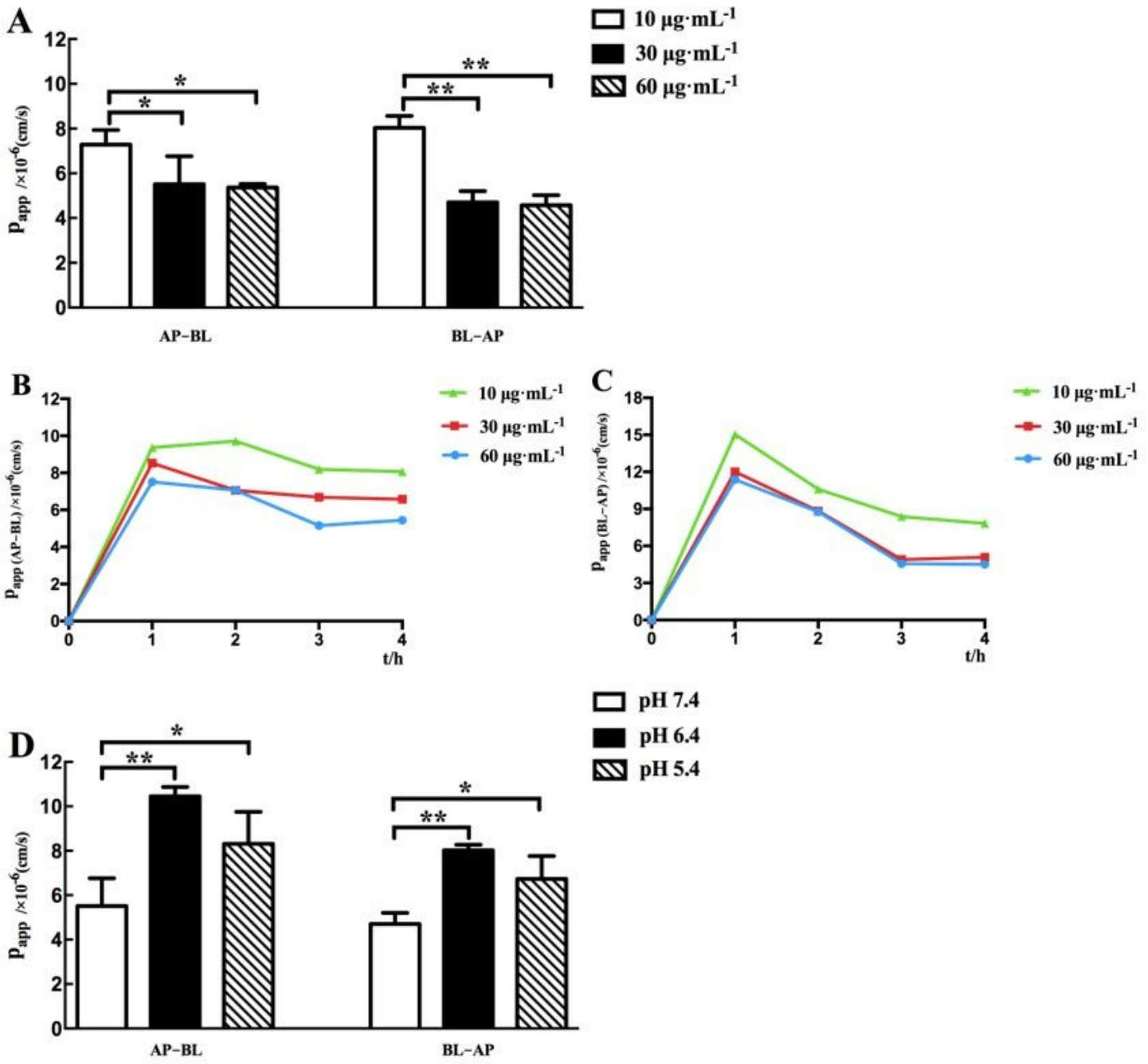

Figure 3

Characterization of the Intestinal Permeability Features of TSG in Caco-2 Cell Monolayer. (A) Bidirectional transport studies of TSG at different drug concentrations (10, 30 and 60 μg·mL-1, respectively). $p < 0.05$ (*), $p < 0.01$ (**), comparison with the group at 10 μg·mL-1 TSG. (B) The apparent permeability (Papp, cm/s) values of AP-BL at 1, 2, 3 and 4 h for TSG. (C) The apparent permeability (Papp, cm/s) values of BL-AP at 1, 2, 3 and 4 h for TSG. (D) The Papp of TSG at different pH values (7.4, 6.4 and 5.4, respectively). $p < 0.05$ (*), $p < 0.01$ (**), comparison with the pH 7.4 group. All results are expressed as mean ± SD (n = 3).

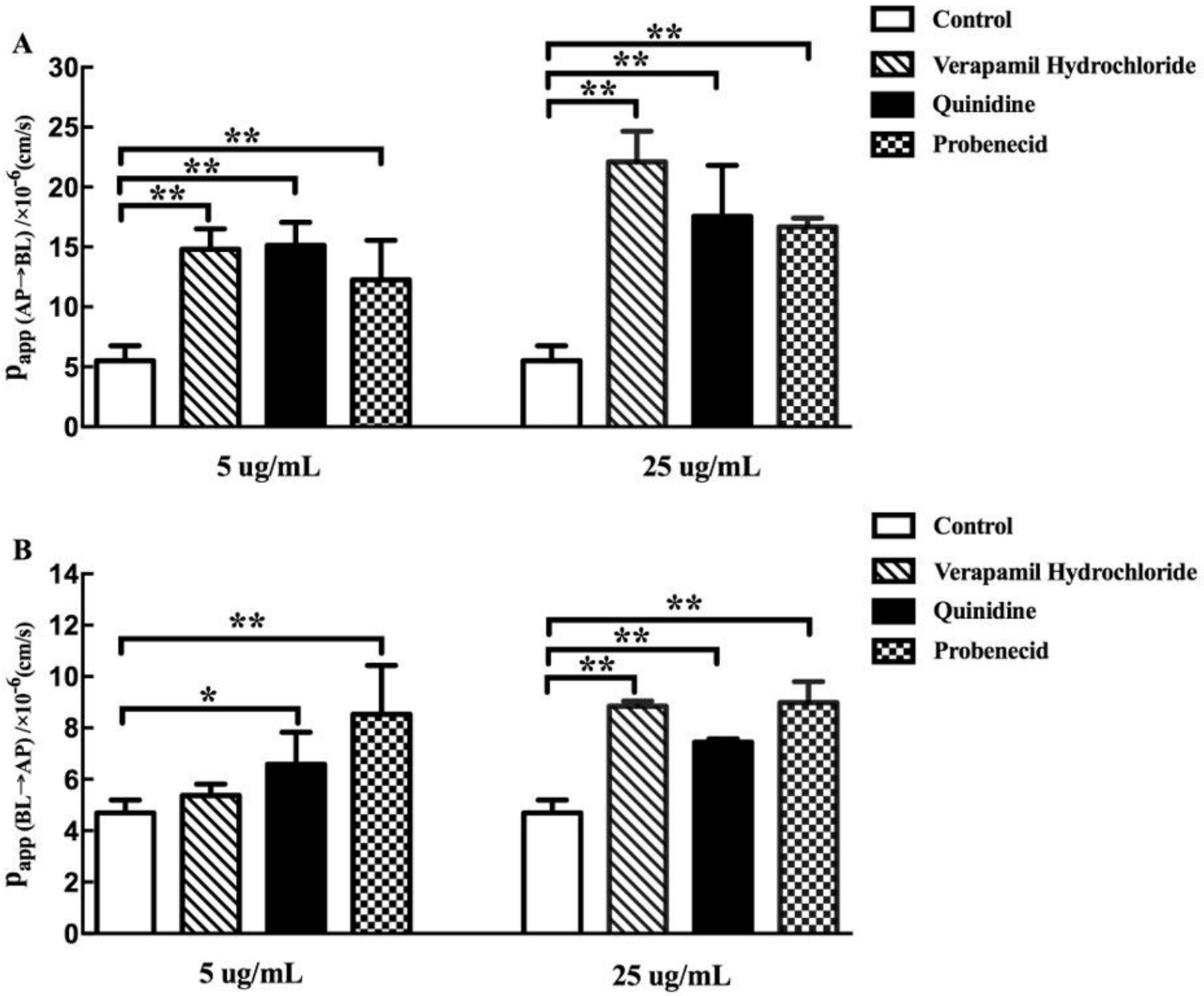

Figure 4

Effect of different inhibitors on the transport of TSG across Caco-2 cell monolayer. The data are presented as the apparent permeability (Papp, cm/s). Effect of P-glycoprotein (P-gp) inhibitor (verapamil hydrochloride and probenecid) and multidrug resistance-associated protein 2 (MRP2) inhibitor (probenecid) on Caco-2 cell monolayer for TSG. AP-BL side (A); BL-AP side (B). $p < 0.05$ (*), $p < 0.01$ (**), comparison with control. All results are expressed as mean ± SD (n=3).

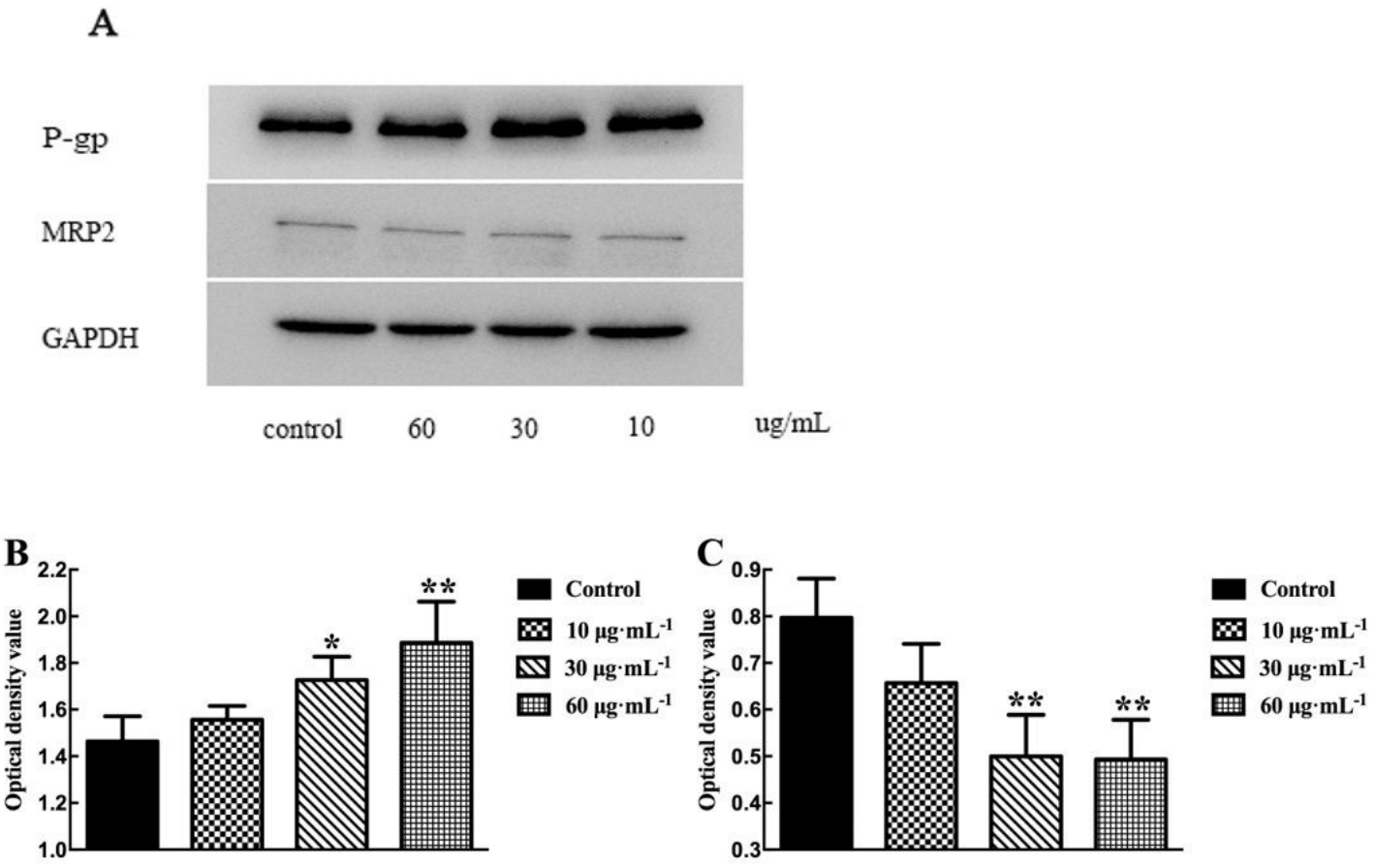

Figure 5

Effects of TSG on the expression of P-gp and MRP2 in Caco-2 Cell Monolayer. (A) The effects of TSG on the expression of P-gp and MRP2. (B) The expression of P-gp in Caco-2 cell after treat with TSG. (C) The expression of MRP2 in Caco-2 cell after treat with TSG. $p < 0.05$ (*), $p < 0.01$ (**), comparison with control. All results are expressed as mean ± SD (n=3).

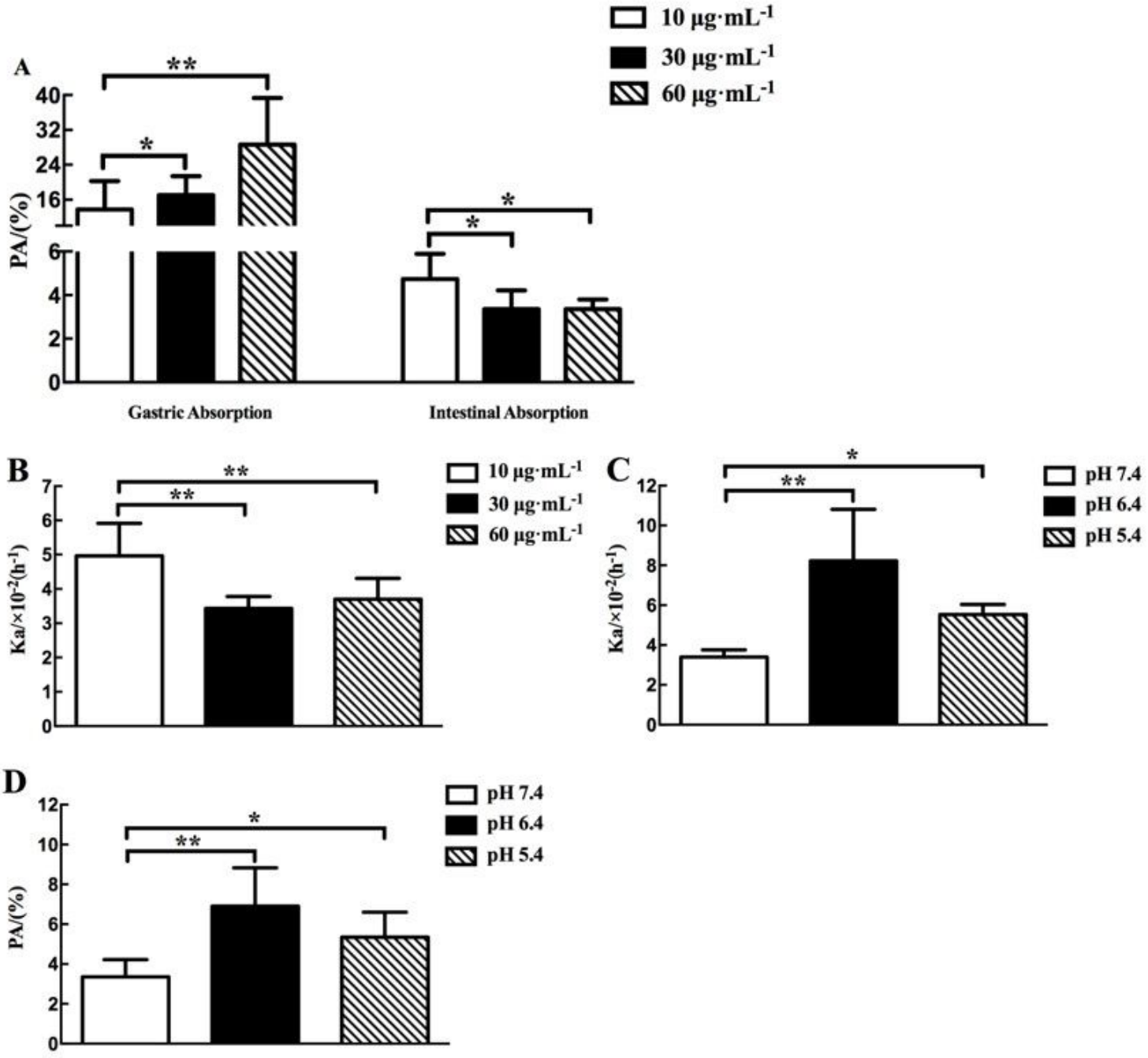

Figure 6

Characterization of the intestinal permeability features of TSG in single-pass intestinal perfusion model. The data are presented as absorption rate constants (Ka, h-1) values and percentage of absorption (PA, %) values. (A) Absorption of TSG in the stomach and small intestine. (B) The absorption rate constants (Ka, h-1) values of TSG at different drug concentrations. $p < 0.01$ (**), comparison with the group at 10 μg·mL-1 TSG. (C) The absorption rate constants (Ka, h-1) values of TSG at different pH values. $p < 0.05$ (*), $p < 0.01$ (**), comparison with the group at pH 7.4. (D) The percentage of absorption (PA, %) values of TSG at different pH values. $p < 0.05$ (*), $p < 0.01$ (**), comparison with the group at pH 7.4. All results are expressed as mean ± SD (n=6).

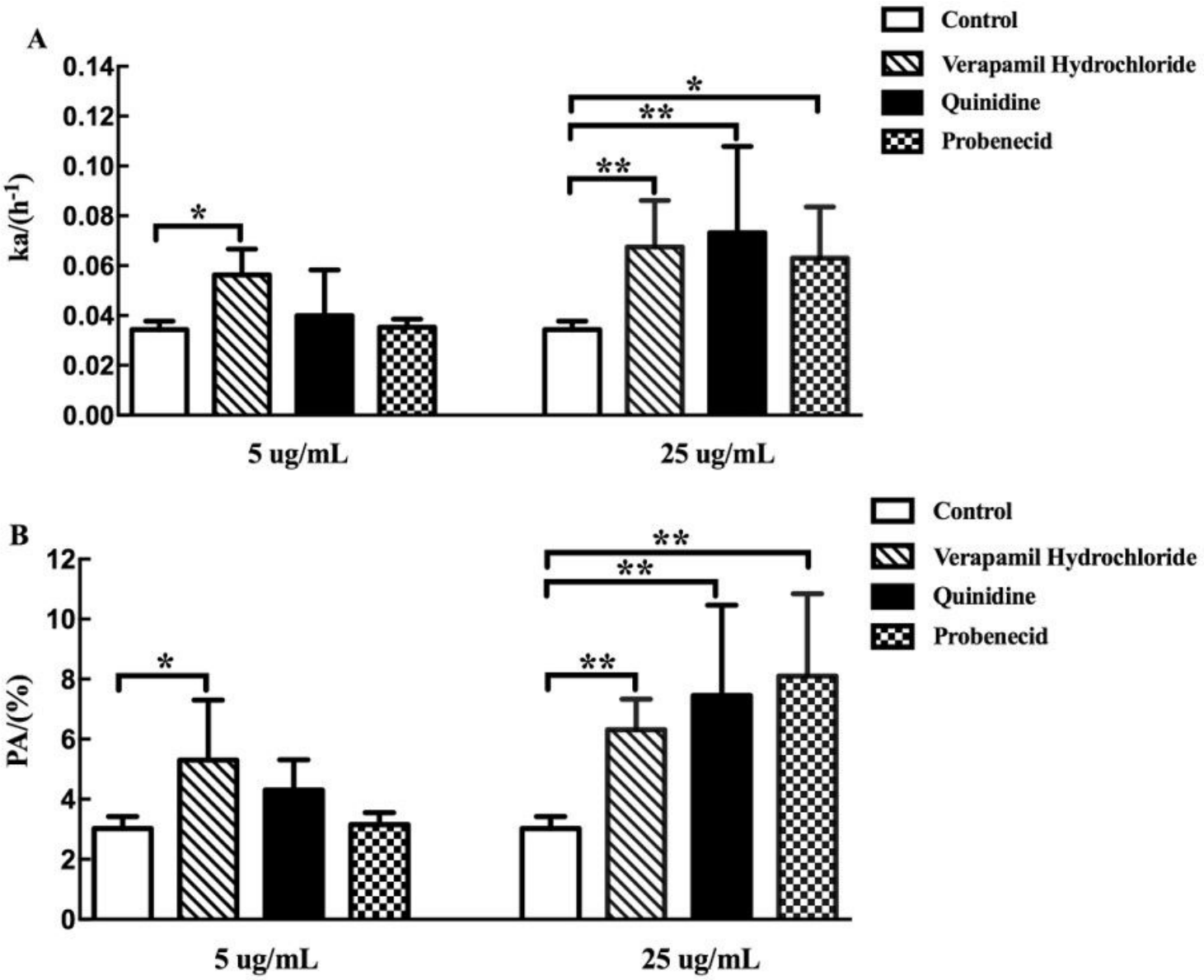

Figure 7

Effect of different inhibitors on intestinal permeability of TSG in rats. The data are presented as absorption rate constants (Ka, h-1) values and percentage of absorption (PA, %) values. Effect of P-glycoprotein (P-gp) inhibitor (verapamil hydrochloride and probenecid) and multidrug resistance-associated protein 2 (MRP2) inhibitor (probenecid) on small intestinal absorption of TSG. Absorption rate constants (Ka, h-1) values (A); Percentage of absorption (PA, %) values (B). $p < 0.05$ (*), $p < 0.01$ (**), comparison with control. All results are expressed as mean ±SD (n=6).

Supplementary Files

This is a list of supplementary files associated with this preprint. Click to download.

- eq2.jpg